BACHELOR THESIS

THE DESIGN AND ANALYSIS OF AN ONBOARD CONTROL SYSTEM OF A TETHERLESS MINIATURE MAGNETIC ROBOT

Isabel Toebes

ENGINEERING TECHNOLOGY –BIOMECHANICAL ENGINEERING
SURGICAL ROBOTICS LAB

EXAMINATION COMMITTEE
Dr. Islam S. M. Khalil
Dr. Arturo Susarrey Arce
Dr. Janset Dasdemir

DOCUMENT NUMBER
BE - 961

UNIVERSITY OF TWENTE.

27-09-2023

CONTENTS

The design and analysis of an onboard control system of a tetherless miniature magnetic robot

Isabel Toebes
Supervisors: Dr. Islam S. M. Khalil, dr. Arturo Susarrey Arce
Surgical Robotics Lab - University of Twente

I. Abstract

Unthethered microelectromechanical systems (MEMS) have a lot of potential for future medicine, for example, restoring blood flow in clogged vessels. This can be done by a MEMS with full energetic autonomy in a static magnetic field, using time-varying current through coils to create mechanical torque, creating a screwing translational movement. In this work, the onboard control system of this MEMS is designed by creating an electrical circuit, which should comply with the set specifications; creating a time-controlled magnetic moment at the frequency of 5 Hz with a phase-shift of 180 degrees between the two coils with a root mean square (RMS) current of 100 mA. The circuit consists of an oscillator, phase shifter, amplifyer stage and two coils. This has first been simulated in LTspice XVII, after which the circuit was built and physically tested. From this a RMS current of 109.3 mA and 100.1 mA have been measured, creating an efficiency of 10.5% and 5.38% for the simulation and physical circuit, respectively.

Keywords: ***MEMS, tetherless miniature magnetic robot, static magnetic field, control system***

1. Introduction

The formation of blood clots to prevent external bleeding is essential for the preservation of the blood inside the body. However, this blood clotting cascade can also be triggered inside the body by pathological thrombosis.[1] If these internal blood clots rupture, they can prevent blood flow through tissues, leading to embolisms. These embolisms can, if located in the cerebral arteries, cause ischemic strokes,[2] which contribute to a total of 5.83% of the total amount of global deaths.[3]

An untethered microelectromechanical system (MEMS) can have the potential to navigate through bodily fluids and engage with blood clots, making it possible to restore blood flow in clogged vessels. This MEMS, as shown in figure 1, would rotate using a constant external magnetic field, using a time-controlled magnetic moment created by coils in the MEMS. This in contrast to using a rotational external magnet, which has the downside of having to move around a patient, which gives it less freedom to move. On top of that has an onboard control system the advantage of combining it with other sensors.

In order to give the MEMS full energetic autonomy, the energy needed to power the coils will be delivered by onboard hydrogen cells. This will create an energy transition from chemical energy to electrical energy to a magnetic moment which will then create a mechanical torque. This can be connected as can be seen in figure 2.

Therefor this paper seeks to answer the question: "How to create a time-varying magnetic dipole moment to create a screwing translational motion of a tetherless miniature robot in a static magnetic field?".

First, the specifications are discussed, after which the design is made and simulated. After this, the design will be physically built and tested, after which the results are discussed.

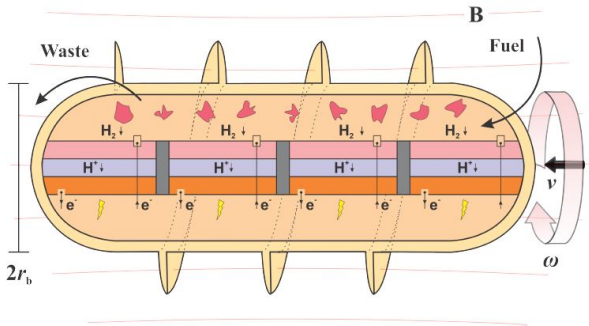

Fig. 1: Schematic representation of the MEMS [4]

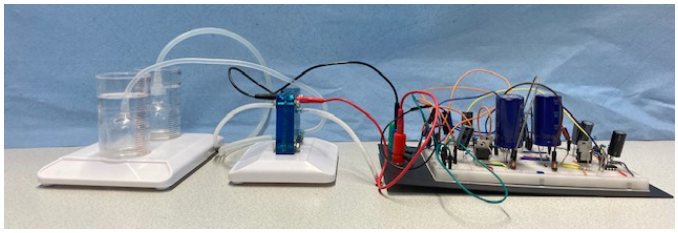

Fig. 2: set-up of the connection of fuel cells to the onboard electronics, consisting from left to right of water, a PEM fuel cell and the onboard control circuit.

2. Design of the onboard control system

In this chapter, the design of the onboard electric circuit is discussed. The purpose of the onboard electronics is to create a sinusoidal current through two coils (SBCP-47HY152B),

with a phase shift of 180 degrees between them. The current through the coils should be enough to create a sufficient magnetic dipole moment to turn the robot around its axis. Firstly, the specifications that need to be met are explained, after which the design is discussed.

A. Specifications of the onboard control system

The frequency of the oscillations should not exceed the turnover frequency of the robot. Under the assumption that the Reynolds number is very small, the turnover frequency **w** can be calculated using formula 1, where **B** is the external magnetic field, r is the radius of the body, and η the viscosity of the fluid. [4]

$$\mathbf{w} = \frac{NS\mathbf{I}_{eff} \times \mathbf{B}}{8r_b^3 \pi \eta} \tag{1}$$

Figure 3 shows the relation between the radius of the body, the current through the coils, I, the turnover frequency, **w**, and the resulting velocity v, visualizing the relationship showed in formula 1. Here it is visible that there is an exponential relationship between the radius of the body and the current needed through the coils, showing that making a slight decrease in size of the MEMS will result in a big decrease in current needed. Downsizing will also have a positive effect on the turn-over frequency, as this has a decreasing exponential relationship with the radius. In order to set the key performance indicators (KPI), the current and turn-over frequency should match the radius of the body. The MEMS should have a radius of 5 mm, therefor in accordance with figure 3, the RMS current through the coils should be at least 60 mA. To create a safety margin, the RMS current is chosen to be 100 mA. At this size, the turn-over frequency will be 11.4 rad/s. As this turn-over frequency is for a viscosity of 200 mPa.s, instead of the 1.0016 mPa.s of water, the turnover frequency will be 362 Hz. The key performance indicators (KPI) are summarized in table I.

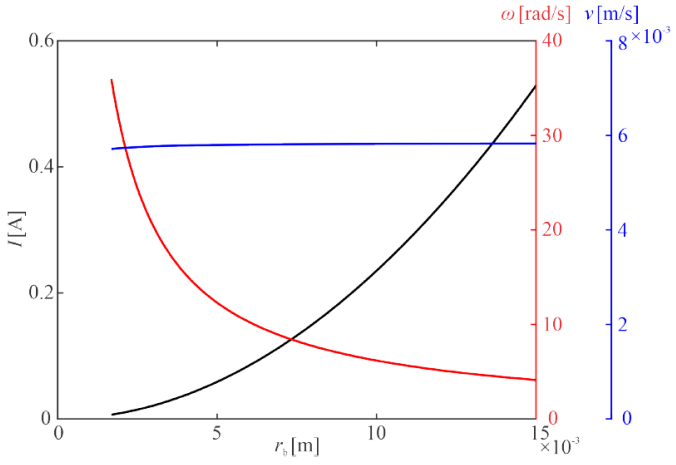

Fig. 3: The radius of the body, r_b plotted against the current through the coils, I, the turnover frequency w and the velocity v. Plotted with the viscosity being equal to 200 mPa.s, the external magnetic field 1.5 T, and ρ equal to 997 $kg.m^{-3}$ [4]

In order to stay well below the turnover frequency, the frequency of the oscillations is chosen to be 5 Hz.

TABLE I: Table containing the KPI of the electronic circuit

Electric KPI	
Inductance of coil [mH]	1.5
DC resistance of coil[Ω]	8
RMS Current through coil [mA]	100
Frequency of time-controlled magnetic moment [Hz]	5
Magnetic KPI	
External electrical fiel [T]	1.5
Mechanical KPI	
Turn-over frequency [Hz]	362
Radius of the body [mm]	5

B. General Overview Circuit

In this chapter, the design of the electric circuit is discussed, which is visible in figure 4. The total circuit consists of five stages; a power supply, the oscillator, a phase splitter, an amplifier stage, and finally the coils.

The first stage is a power supply. The whole system is first tested with two power supplies to create a positive and negative voltage, which is set at plus and minus 3.1 Volt, respectively.

Next is the oscillator stage. Here, the DC signal, provided by the power source, will be converted into an AC signal with a set amplitude and frequency. This is done by using a Wien-Bridge oscillator, as this is a commonly used, easy low-frequency oscillator that can be used for frequencies in the audio frequencies, but also in the sub-audio frequencies, as needed in this circuit.[5][6]

In order to drive two coils with a phase shift of 180 degrees, a single-stage phase-splitter is created, using the characteristic of the common emitter and common collector circuit, where the former stays in phase, while the latter has a phase shift of 180 degrees with respect to the incoming signal.[7] In order to make sure that the signal is not clipped in the phase-splitter, a voltage divider will be placed between the oscillator and phase-splitter to decrease the signal.

Lastly, the signal is amplified first by an opamp (AD823A), from which the current is even further amplified by an AB stage amplifier to increase the current which is then driven through the coils. Here is chosen to use an AB-amplifier stage as this stage has as a balance between efficiency and linearity.[8][9][10]

C. Calculations Circuit

The complete circuit, as visible in figure 4, consist of the stages as mentioned in chapter 1.

Firstly, the system is powered by two power sources, both set to 3.1V. Next is the Wien-bridge oscillator. In order to create the frequency around 5 Hz, in accordance with table I, the value of the resistors $R8$ and $R11$ as visible in figure 4 can be determined to be slightly above 30kΩ, by setting the values of capacitors $C2$ and $C3$ to 1 μF and using formula 2, where f, R and C are the frequency, resistance and capacitance values, respectively.

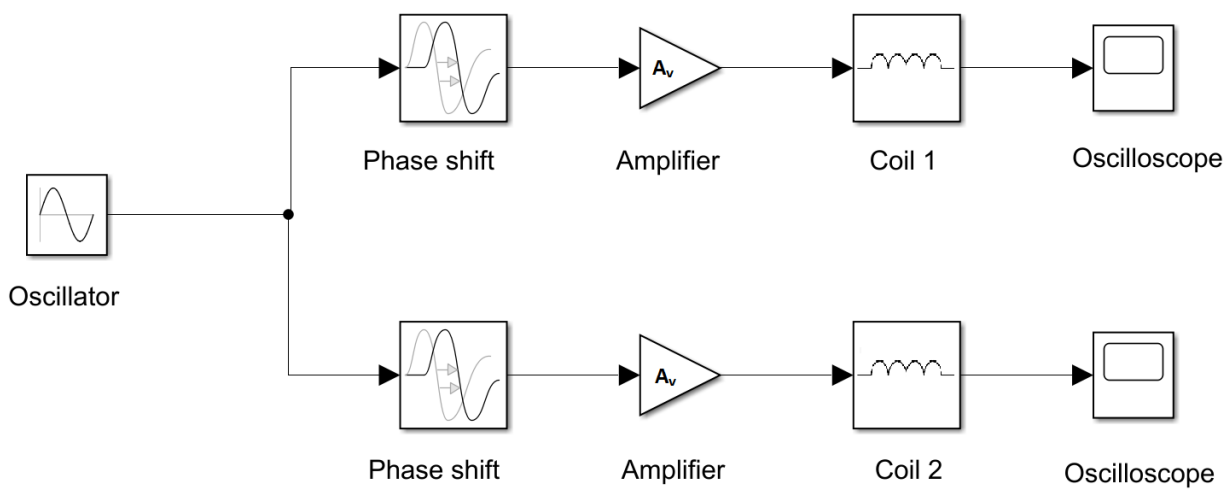

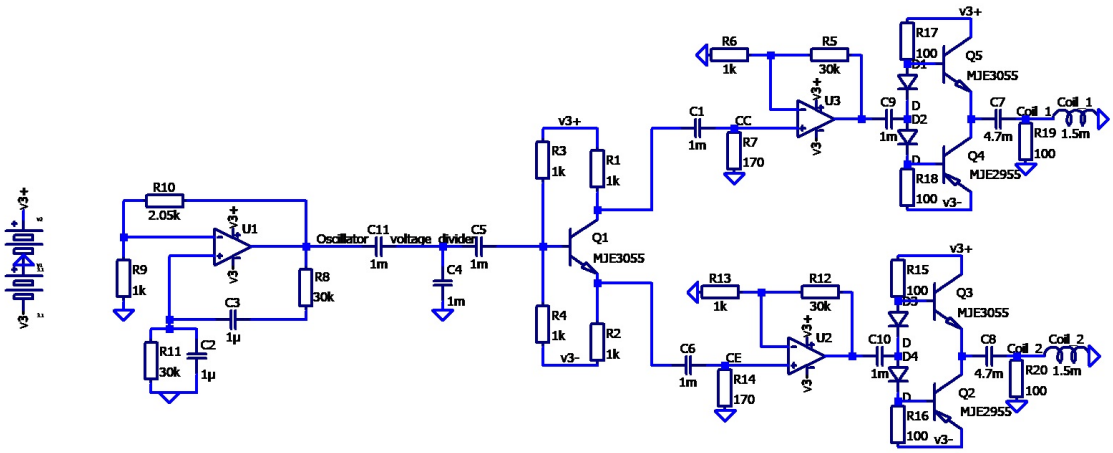

Fig. 4: The complete electronic control circuit visualised (a) as an overview of the circuit and (b) with all electronical component values.

$$f = \frac{1}{2\pi RC} \tag{2}$$

As the total gain of the oscillator should be equal to one, and the feedback factor is equal to $\frac{1}{3}$, the negative feedback gain, created by resistor $R2$ and $R3$ should be equal or bigger than 3.[6] By using formula 3, where A is the gain, and choosing R2 to be 1 kΩ, R3 can be calculated to be equal or higher than 2 kΩ.

$$A = 1 + \frac{R3}{R2} \tag{3}$$

As the opamp $U1$ (NE5534) has no rail-to-rail output, the voltage swing will be lower than 3.1V. The voltage swing should still be smaller for the voltage divider not to clip the signal. Therefor a capacitive voltage divider is implemented, according to formula 4. Hereby choosing the values of $C11$ and $C4$ equal to decrease the signal by a half.

$$V_{out} = \frac{C11}{C4 + C11} V_{in} \tag{4}$$

This is now connected to the phase splitter stage by a coupling capacitor $C5$. The phase splitter needs to be biased

by resistors $R3$ and $R4$. These two resistors act as a voltage divider, which should center the DC voltage around 0V. Therefore both resistors should have the same value, so these have been chosen to be 1kΩ.[11]

Resistors $R1$ and $R2$ determine the gain of the common emitter and the common collector. As the two signals should have the same amplitude, the resistors should have the same values. Therefore they have both been chosen to be 1kΩ. Now both the common collector and common emitter are connected to their own amplifier stages.

The phase splitter and amplifier stage are connected by a high-pass filter to remove the DC bias from the signal.[11] Therefore the high-pass filter is designed to allow frequencies higher than 1 Hz to pass through, by using formula 5 and setting $C1$ and $C6$ to 1mF, $R7$ and $R14$ can be calculated to be around 160Ω.

$$f_c = \frac{1}{2\pi RC} \tag{5}$$

The signal is then amplified with opamps (AD823A) $U2$ and $U3$ with a gain of 30, created by resistor pair $R5$ and $R6$ and pair $R12$ and $R13$. This is then connected with a coupling capacitor to a current amplifying stage, to amplify the current further than the opamp is able to do. This AB-amplifier stage is biased by diodes $D1$ to $D4$ and resistors $R15$ to $R18$. The diodes create thermal stability and a voltage drop of about 0.65V required for the transistors. After this, a capacitor, $C7$ and resistor $R19$ are used as a low-pass filter to remove the DC signal from the AC signal.[11] To make sure the frequency of the oscillation is not damped, the cut off frequency is set at 0.33 Hz. Using formula 5, the values of the resistor and capacitor can be determined.

D. Simulations

The design is simulated in LTspice $XVII$. Firstly, the behavior of the oscillator is simulated, which is visible in figure 5a. In blue, the voltage measured after the oscillator is shown, where the amplitude is about 1V and the frequency around 5.3 Hz. The decreased voltage after the voltage divider is visible in red, oscillating at the same frequency.

In figure 5b, the voltage against time of the Common Collector (CC) and Common Emitter (CE) is visible, depicting a phase shift of 180 degrees between the two signals.

Then, the voltage over the coils is depicted in figure 5c. Here is visible that the voltage is not a perfect sinusoidal anymore. Finally, the current through the two coils is depicted in figure 5d, where the red and blue both display one of the two coils. As the signal is not a perfect sinusoidal, the peak value is 230 mA to create a RMS value of about 108 mA.

3. METHODS

Now, the circuit is physically build and tested with two power supplies. The positive side of the first power supply is connected to the negative side of the other and will create the ground of the circuit. Now, the other terminals of the power supplies will create a positive voltage and a negative voltage. This is connected to the circuit. Using an oscilloscope, the voltage over the coils can be measured and visualized. The current through the coils can be calculated using Ohms law and the impedance of the coil. The latter consists of the inductive reactance and the resistance of the coil, and can be determined by formula 6, where R and X_L are the resistance and the inductive reactance, respectively.

$$Z = \sqrt{R^2 + X_L^2} \tag{6}$$

The inductive reactance can be determined by formula 7, with f the frequency of the oscillations and L the inductance of the coil.

$$X_L = 2\pi f L \tag{7}$$

When the current through the coils has been determined, can the magnetic moment, M, be calculated with formula 8, where I_{RMS}, N and A, are the RMS current through the coil, the amount of windings and the surface of the coil, respectively.

$$M = I_{RMS} N A \tag{8}$$

The efficiency of the circuit can be calculated by determining the power input and the power output. The input current is given by the power supply, from which the power can be calculated with the chosen voltage, using formula 9, where U and I are the voltage and current, respectively.

$$P = UI \tag{9}$$

By measuring the voltage and current over the coils, the output power can also be calculated with formula 9. From this, the efficiency of the circuit can be calculated by dividing the output power by the input power.

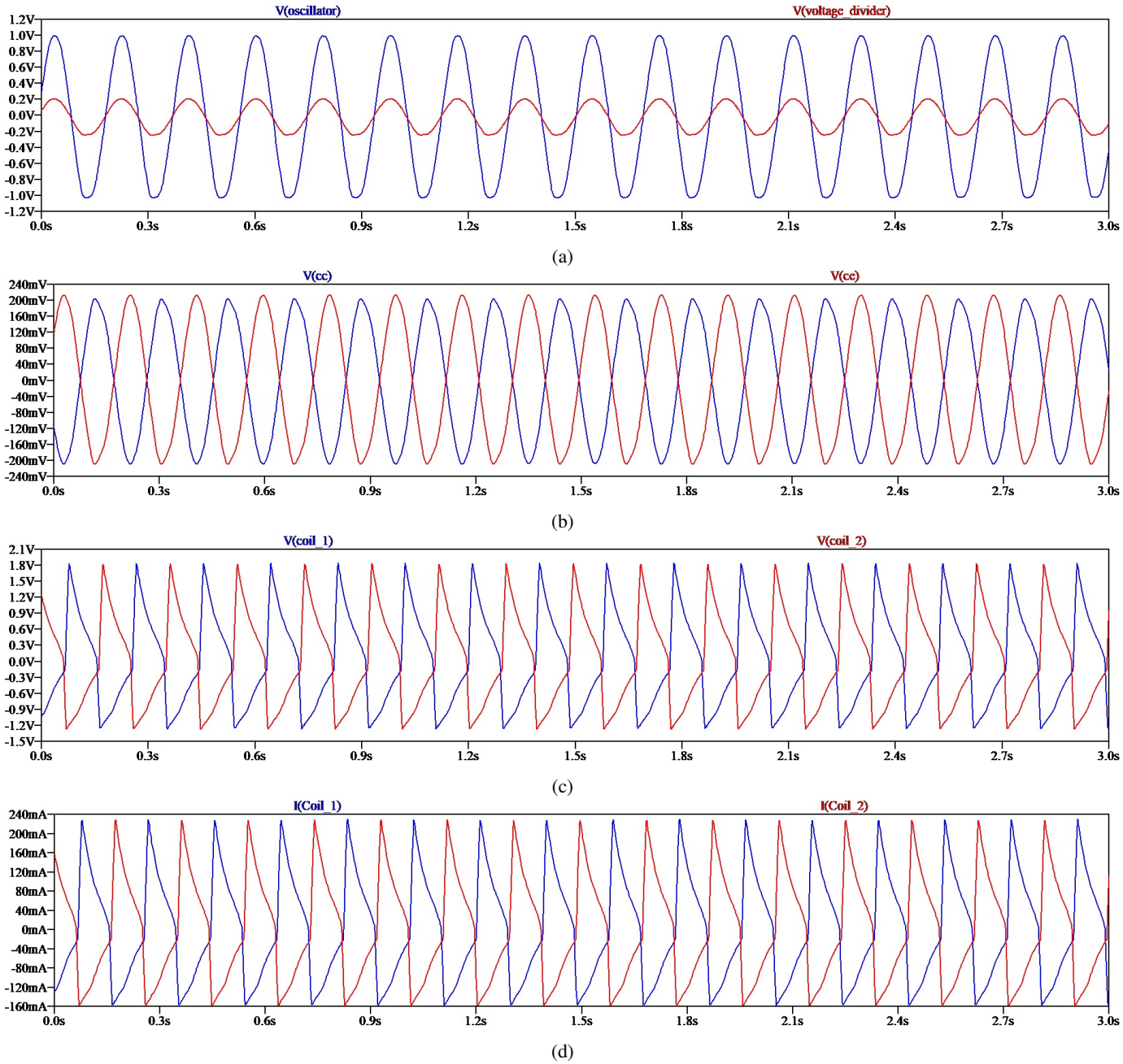

Fig. 5: The simulations of the designed onboard electronic circuit showing the (a) AC voltage created by the oscillater and the decreased voltage after the voltage divider, (b) phase difference of 180 degrees between the common collector and common emitter voltage, (c) the voltage across the two coils and (d) the current through the two coils.

4. Results

In this section, the results of the experiments are shown. The measured voltage over the two coils is depicted in figure 6a. Given that the coils have an impendance of 8 Ω, the current can be calculated, which is depicted in figure 6b, showing an imperfect sine wave reaching up to 220 mA. The sine wave remains the same over time, having barely variations in the peaks. From this, the RMS current can be calculated, which is on average 100.1 mA.

From the RMS current of the peaks, the RMS magnetic moment can be calculated, which will be 0.147 mJT^{-1}. From the current through the coils, the average power can be calculated as described in 3. This will give an average power of 159.1 mW.

The power supplies supply a current of 0.522 A and 0.486 A at a voltage of 3.1V. This creates 2.9551 W that is supplied to the circuit. From this, the efficiency can be calculated to be 5.38%.

This all has been summarized in table 6, where the results from the experiment are placed next to the results of the simulation.

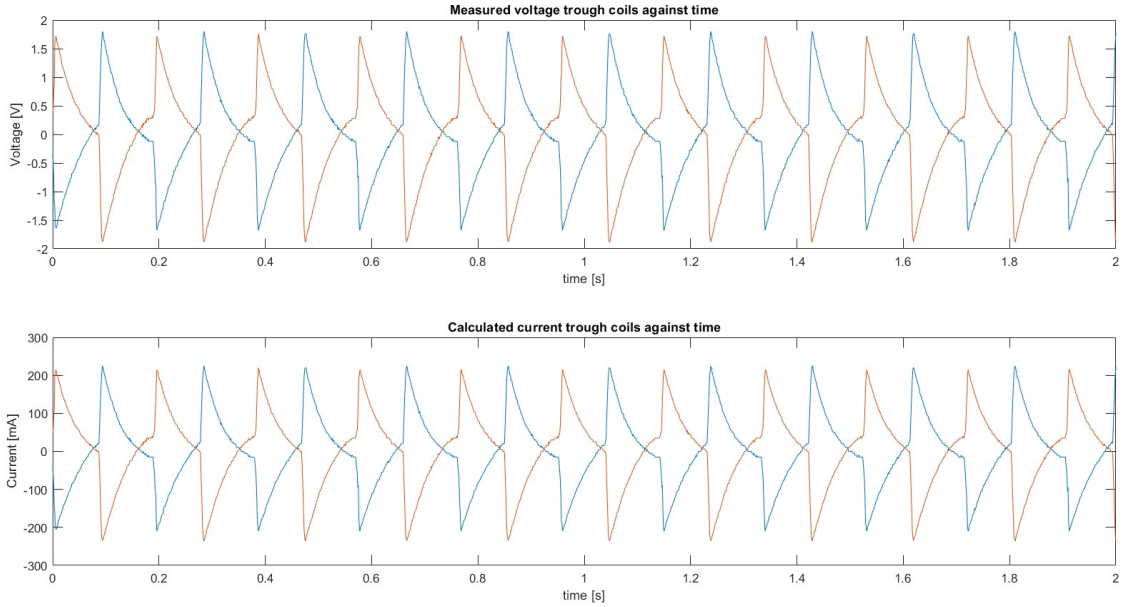

Fig. 6: Experimental results of the a) voltage through the coils and b) the current through the coils against time

TABLE II: Results of the simulation and the experiment showing the behavior of the system.

	Simulation	power supply
RMS current [mA]	109.3	100.1
Magnetic moment [mJ/T]	0.161	0.147
Average Power out [mW]	191.15	159.1
Average Power in [W]	1.8164	2.9551
Efficiency [%]	10.5	5.38

5. Discussion

In figure 6 is visible that the current through the coils has a phase shift of 180 degrees and a frequency of 5.3 Hz. The RMS current through the coils is 100.1 mA, complying with the specifications. The size of the circuit does not yet fit inside a miniature robot with a radius of 5mm and should be further downsized.

As visible in table II, the results with the real-life experiments resemble the results of the simulation to a certain extent. The RMS current is slightly lower, which can be due to slight fabrication deviations from the component values, but also due to uncertainties in measuring the voltage across the coils.
The voltage and current through the coils are not a perfect sinusoid, this is due to the fact that the supply voltage is too low to amplify the whole signal, creating a clipped signal after opamps $U2$ and $U3$. In order to create a less clipped signal, the power supply should be increased.
As the whole circuit uses quite a lot of current, the system cannot be powered by small coin-sized batteries, as these provide too little current to power the entire circuit.
The whole electronic circuit is made on a breadboard, which can introduce more noise to the signal. This can be decreased by soldering the whole system.
The total circuit has a relatively low efficiency, which can due to the fact that in coils, there is a phase shift between the current and the voltage. This phase shift creates a lower power output, therefor resulting in a lower efficiency.

A. *Further research*

The onboard circuit is not ready yet to connect to either batteries or fuel cells, on which further research can be focused, so this can be connected together. In addition, the circuit is made on a breadboard and should be downsized in order to fit in the MEMS, and fit the specification of the MEMS having a radius of 5 mm.

6. Conclusion

In this paper, the onboard circuit control system of a untethered mini robot has been designed. The purpose of the circuit is to create sinusoidal current of 100 mA through two coils with a phase shift of 180 degrees, to create a time-controlled magnetic moment. With exception of the size requirement, are the specifications as set in table I met, creating a time-controlled magnetic moment.

References

[1] S. A. Smith, R. J. Travers, and J. H. Morrissey, "How it all starts: initiation of the clotting cascade," *Crit. Rev. Biochem. Mol. Biol.*, vol. 50, no. 4, p. 326, 2015. DOI: 10.3109/10409238.2015.1050550.

[2] V. Tutwiler, J. Singh, R. I. Litvinov, J. L. Bassani, P. K. Purohit, and J. W. Weisel, "Rupture of blood clots: Mechanics and pathophysiology," *Sci. Adv.*, vol. 6, no. 35, Aug. 2020. DOI: 10.1126/sciadv.abc0496.

[3] K.-S. Huang, D.-X. He, Q. Tao, *et al.*, "Changes in the incidence and prevalence of ischemic stroke and associations with natural disasters: an ecological study in 193 countries," *Sci. Rep.*, vol. 12, no. 1808, pp. 1–8, Feb. 2022, ISSN: 2045-2322. DOI: 10.1038/s41598-022-05288-7.

[4] E. van Renselaar, B. Keitel, M. Dinc, *et al.*, "Scaling Rules for Microrobots with Full Energetic Autonomy," in *2022 International Conference on Manipulation, Automation and Robotics at Small Scales (MARSS)*, IEEE, Jul. 2022, pp. 1–6. DOI: 10.1109/MARSS55884.2022.9870509.

[5] Y. L. I. and J. Hou, "An Electrical-Variable-Frequency Compact Wien-Bridge Oscillator," *Wuhan Univ. J. Nat. Sci.*, vol. 27, no. 3, pp. 261–264, Jun. 2022, ISSN: 1007-1202. DOI: 10.1051/wujns/2022273261.

[6] R. Mancini and R. Palmer, "Sine Wave Oscillators," in *Op Amps for Everyone (Third Edition)*, Newnes, Jan. 2009, pp. 341–363, ISBN: 978-1-85617-505-0. DOI: 10.1016/B978-1-85617-505-0.00019-3.

[7] A.-J. Annema, *Electronics*. Enschede: Electrical Engineering - University of Twente, 2022.

[8] R. Bortoni, S. N. Filho, and R. Seara, "On the design and efficiency of class A, B, AB, G, and H audio power amplifier output stages," *Journal of the Audio Engineering Society. Audio Engineering Society*, vol. 50, no. 7, pp. 547–563, Jul. 2002, ISSN: 0004-7554. [Online]. Available: https://www.researchgate.net/publication/290528247_On_the_design_and_efficiency_of_class_A_B_AB_G_and_H_audio_power_amplifier_output_stages.

[9] M. El-Dakroury, "Design and analysis of class AB RF power amplifier for wireless communication applications," en,

[10] R. A. R. van der Zee, "High efficiency audio power amplifiers: design and practical use," *University of Twente Research Information*, May 1999. [Online]. Available: https://research.utwente.nl/en/publications/high-efficiency-audio-power-amplifiers-design-and-practical-use.

[11] M. Jones, "Chapter 2 - Basic Building Blocks," in *Valve Amplifiers (Fourth Edition)*, Newnes, Jan. 2012, pp. 65–154, ISBN: 978-0-08-096640-3. DOI: 10.1016/B978-0-08-096640-3.00002-2.